

Folic acid functionalized ZnO quantum dots for targeted cancer cell imaging

This content has been downloaded from IOPscience. Please scroll down to see the full text.

2015 Nanotechnology 26 305702

(<http://iopscience.iop.org/0957-4484/26/30/305702>)

View [the table of contents for this issue](#), or go to the [journal homepage](#) for more

Download details:

IP Address: 222.66.115.230

This content was downloaded on 09/07/2015 at 00:55

Please note that [terms and conditions apply](#).

Folic acid functionalized ZnO quantum dots for targeted cancer cell imaging

Ying-Ying Ma, Hui Ding and Huan-Ming Xiong

Department of Chemistry, Fudan University, Shanghai 200433, People's Republic of China

E-mail: hmxiong@fudan.edu.cn

Received 6 April 2015, revised 23 May 2015

Accepted for publication 9 June 2015

Published 7 July 2015



CrossMark

Abstract

Aqueous stable luminescent ZnO quantum dots (QDs) were successfully synthesized with primary amine groups on the surface, which were designed to conjugate with folic acid (FA) to produce the final ZnO-FA QDs. Such ZnO-FA QDs were able to target some specific cancer cells with overexpressed FA receptors on the membranes and thus differentiate the MCF-7 cancer cells from the normal 293T cells. The nanoparticle uptaking experiments by different cells were carried out in parallel and tracked by confocal laser microscopy dynamically. The results confirmed the specificity of our ZnO-FA QDs towards the FA-receptor overexpressed cancer cells, which had potential for diagnosing cancers *in vitro*.

Keywords: ZnO, quantum dots, folic acid, cancer cells, fluorescent imaging

(Some figures may appear in colour only in the online journal)

1. Introduction

Cancers are seriously threatening human health [1, 2], but early diagnosis techniques are deficient, and the clinical therapy methods against cancers are inefficient at present. Fortunately, during numerous investigations concerning cancers in recent decades, researchers have found many special receptors on cancer cell surfaces [3–8] that can be utilized to import the label molecules or drugs with the targeting groups. For example, there are plenty of folic acid (FA)- α receptors on the surfaces of epithelial ovarian cancer cells that can be labeled by FA-functionalized fluorescent agents so that the tumor-specific fluorescence imaging can supply great assistance in human ovarian cancer surgery [9]. In fact, FA receptors are overexpressed on cancer cell membranes in the ovary, endometrium, kidney, lung, breast, and so on, but exist at low levels on the normal cells [10–13]. Thus, FA groups are widely modified onto various fluorescent materials like organic dyes, gold nanoclusters [14, 15], semiconductor quantum dots (QDs) [16, 17], and rare earth nanoparticles [18, 19] for detection of cancer cells both *in vivo* and *in vitro*. Due to the high sensitivity and real-time imaging ability of fluorescent techniques, the FA-modified probes can help the rapid diagnosis of cancers when the tissue slices are analyzed *in vitro*. Therefore, preparing highly efficient fluorescent

probes that can differentiate between cancer cells and normal cells is an urgent task in front of researchers.

Photoluminescent ZnO QDs have been reported in many biological studies, such as cell imaging [20, 21], drug delivery [22, 23], animal experiments [24, 25], and antibacterial agent [26–28]. As a kind of fluorescent probe, ZnO QDs are much more stable than organic dyes, especially under ultraviolet (UV) light; they are almost nontoxic in comparison with the classical CdSe/CdTe QDs, and they are much smaller and cheaper than the popular rare earth-based nanoparticles. Hence, developing ZnO-based nanoprobe is possible to push forward the fluorescent probes for future industrialization. However, ZnO fluorescence mainly arises from the surface defects, which are sensitive towards the chemical environment. Water, acids, some transition metal ions, and strong organic ligands are able to quench ZnO fluorescence [29]. To obtain aqueous ZnO QDs with special groups, the synthetic routes and surface modifications should be carried out critically. So far, the FA-functionalized ZnO QDs are rarely seen in the literature, and their successful application to cancer cells remains a challenge.

In this work, we designed a new route to synthesize water-stable ZnO@polymer core-shell QDs (ZnO-NH₂), which had amine groups on the external shells. Then FA was conjugated onto the ZnO surface as a targeting moiety through the reactions between FA and amine groups to

produce the final ZnO-FA QDs. Both ZnO-NH₂ and ZnO-FA QDs were characterized carefully, and they showed stable yellow fluorescence in aqueous solutions. Afterwards, they were incubated with two kinds of cells, respectively: the human breast carcinoma cells MCF-7 and the human embryonic kidney cells 293T. By the fluorescence imaging technique under a confocal laser scanning microscope (CLSM), we found the cellular uptake process of ZnO-FA QDs by MCF-7 cells was much more significant than those of two other control groups, ZnO-FA/293T and ZnO-NH₂/MCF-7, which verified the specific targeting ability of ZnO-FA QDs towards MCF-7 cells.

2. Materials and methods

2.1. Materials

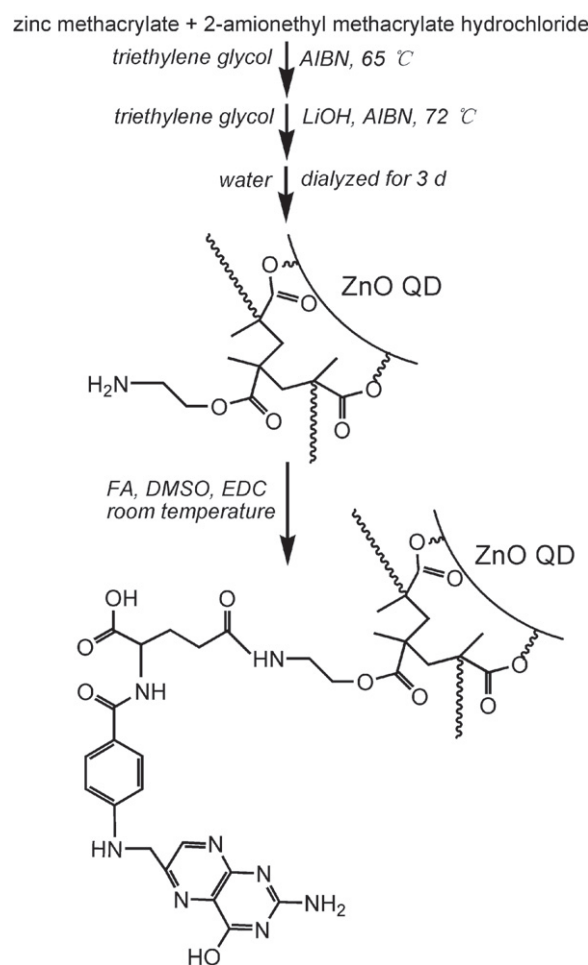
Lithium hydroxide (LiOH · H₂O), zinc oxide (ZnO), methacrylic acid, and triethylene glycol (TEG) 2, 2'-azobisisobutyronitrile (AIBN) were obtained from Sino-pharm Chemical Reagent Co., Ltd (Shanghai, China). 2-Amionethyl methacrylate hydrochloride and 3-[4, 5-dimethylthiazol-2-yl]-2, 5-diphenyltetrazolium bromide (MTT) were obtained from Sigma-Aldrich. All chemical reagents were of analytical grade and used as received.

2.2. Synthesis of the ZnO-NH₂ QDs

25 g of methacrylic acid was dissolved in 100 mL of deionized water and heated to 60 °C, and then 12.5 g of ZnO powder was added into the solution to get zinc methacrylate. Subsequently the solution was evaporated by rotary evaporator to be solid zinc methacrylate then dehydrated in a vacuum oven at 80 °C for 24 h. 0.05 g of 2, 2'-azobisisobutyronitrile (AIBN) and 20 mL of 0.05 M 2-Amionethyl methacrylate hydrochloride triethylene glycol solution were dissolved in 20 mL of 0.05 M zinc methacrylate triethylene glycol solution. The solution was stirred and heated at 65 °C for 10 min. Then another 0.05 g of AIBN and 20 mL of 0.1 M LiOH triethylene glycol solution were added into the reaction system and kept stirring at 72 °C for 1 h. After cooling down to room temperature, the solution was dialyzed against deionized water for 3 d to obtain the purified ZnO-NH₂ QDs.

2.3. Synthesis of folic acid-conjugated ZnO QDs

To modify FA onto ZnO QDs, 1 mg of FA was dissolved in 0.5 mL of dimethyl sulfoxide (DMSO), then 1 mg of 1-(3-dimethylaminopropyl)-3-ethylcarbodiimide hydrochloride (EDC) was added and stirred for 30 min. Afterwards, 15 mL of ZnO-NH₂ QDs aqueous solution was added into the reaction mixture and stirred overnight at room temperature. The obtained solution was dialyzed against deionized water for 2 d to obtain the final ZnO-FA QDs.



Scheme 1. Synthetic route of the ZnO-FA QDs.

2.4. Characterization

Various instruments were employed to characterize the ZnO QDs. The transmission electron microscopy (TEM) images were obtained from a Tecnai G2 F20 S-twin field emission transmission electron microscope. The x-ray diffraction (XRD) patterns were collected at room temperature using a Bruker D4 Endeavor x-ray diffractometer with Cu-K α radiation ($\lambda=0.1541$ nm, 40 kV). The dynamic light scattering (DLS) spectra and zeta potentials were measured on a Malvern ZS-90 Zetasizer. The UV-vis absorption data were recorded by a Unico 2802 UV/Vis spectrometer. The Fourier transform infrared spectra were recorded on a Perkin Elmer Avatar 360 E. S. P. FTIR spectrometer in a range of 4000 ~ 400 cm⁻¹, using the KBr pellet method. The PL spectra were recorded by a Horiba JobinYvon fluoromax-4 spectrofluorometer.

2.5. Cell viability assay

Typical thiazolyl blue tetrazolium bromide (MTT) assays were applied in cytotoxicity evaluation for MCF-7 cells. Cells were seeded at 7×10^3 cells per cell into a 96-well cell culture plate in an incubation medium (DMEM) with 10% FBS at 37 °C and with 5% CO₂ for 24 h. Then the cells were

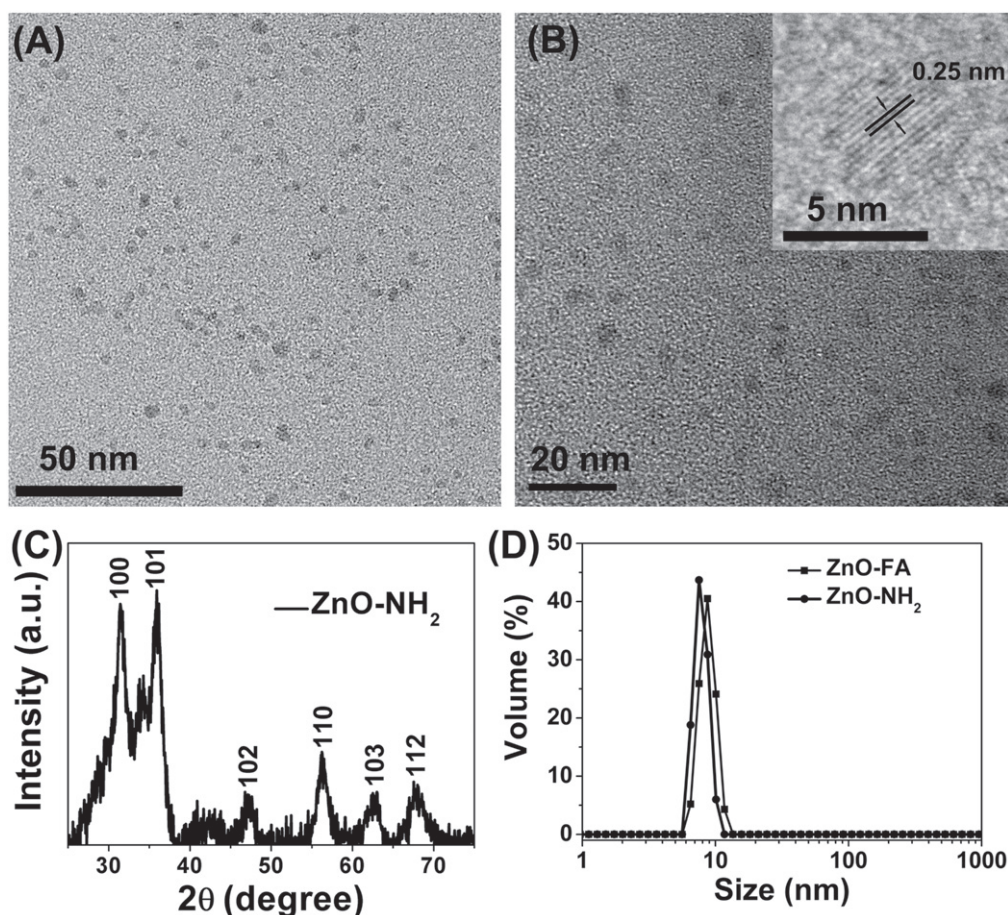


Figure 1. TEM images of (A) ZnO-NH₂ and (B) ZnO-FA. The inset shows the HRTEM of a single particle. (C) X-ray diffraction patterns of ZnO-NH₂ powder. (D) DLS data of ZnO-NH₂ and ZnO-FA QDs in water.

incubated with various concentrations of ZnO-NH₂ QDs and ZnO-FA for 24 h, respectively. Finally, the formazan crystals were dissolved in DMSO, and the absorbance of MTT at a wavelength of 492 nm was measured by an automatic ELISA analyzer.

2.6. Cell imaging experiments

Before the confocal fluorescent imaging, MCF-7 cells and 293T cells were cultured on 35 mm glass-based culture dishes at a density of 5×10^4 cells/mL in DMEM for 24 h. ZnO-NH₂ QDs and ZnO-FA NPs were added into the incubation medium at the Zn²⁺ concentration of $10 \mu\text{g mL}^{-1}$ for different incubation periods in 5% CO₂ at 37 °C. Then the cover glasses were visualized by an Olympus IX2-DSU disk scanning confocal microscope.

3. Result and discussion

In order to obtain aqueous ZnO QDs, various modifications like organic ligands [30], inorganic shells [31], and polymer coatings [20] have been investigated in recent decades. Here we designed copolymer shells for ZnO QDs, and the synthetic route is shown in scheme 1. First, ZnO@polymer core-shell

QDs (ZnO-NH₂) were synthesized through a two-step copolymerization method, according to our previous invention. In the present work, a new monomer with amine group, 2-amionethyl methacrylate hydrochloride, was employed for copolymerization with ZnO-MAA in the presence of an AIBN initiator. In this way 2-amionethyl methacrylate hydrochloride was bound onto the ZnO surface to get a copolymer shell with the internal hydrophobic polymethacrylate layer and the external hydrophilic amine groups so that the obtained ZnO QDs were modified with amine groups on the surfaces. Secondly, the γ -carboxyl group of FA was activated by EDC and participated in the conjugation with the primary amino groups on the surface of ZnO QDs to produce stable ZnO-FA QDs. Finally, the ZnO-FA QDs were purified by repeated dialyses and dispersed in water homogeneously. The high-resolution TEM (HRTEM) images in figure 1(a) show that the ZnO-NH₂ QDs are uniform and monodispersed with average diameters of about 3.9 nm. After conjugation of FA, the final ZnO-FA QDs are still stably dispersed with ZnO lattice fringes, which are about 0.25 nm, corresponding to the 101 planar spacing of the wurzite structure (figure 1(b)). The powder XRD pattern of ZnO-NH₂ is consistent with the typical ZnO wurzite structure, as shown in figure 1(c), according to the Debye-Scherrer formula $D = 0.89\lambda/\beta\cos\theta$, where λ is the x-ray wavelength

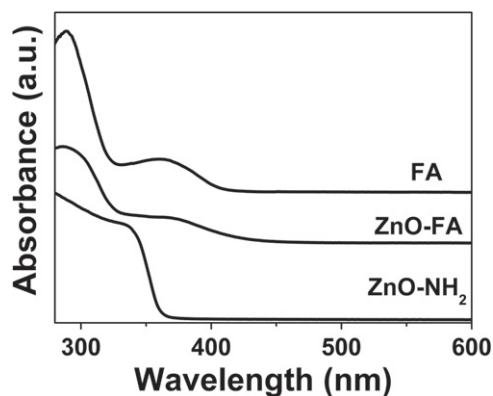


Figure 2. UV-vis absorption curves of FA, ZnO-FA, and ZnO-NH₂ in aqueous solutions.

($K\alpha = 0.154\ 184\ \text{nm}$), β is the Bragg diffraction angle, and θ is the full width at half-maximum of the XRD peak. After calculation, the mean size of the ZnO-NH₂ is 4.8 nm, which is consistent with the HRTEM results. The DLS measurement in figure 1(d) indicates that the ZnO-NH₂ and ZnO-FA QDs had a narrow size distribution around 8 nm. The average hydrated diameters of ZnO-NH₂ and ZnO-FA QDs were 7.5 and 8.7 nm, respectively. The larger diameter observed from DLS included not only the QD's core, but also the hydrated layers adsorbed around ZnO QDs [32].

The UV-vis and the infrared (IR) spectra of FA, ZnO-NH₂, and ZnO-FA samples were compared, respectively, to verify the FA modification on ZnO QDs. The typical absorption bands at 281 and 356 nm for FA [33] are clearly seen in the absorption curve of ZnO-FA (figure 2), indicating that a considerable amount of FA molecules have been grafted onto ZnO QDs successfully. In the meantime, the absorption band at about 340 nm for ZnO-NH₂ also appears in the ZnO-FA curve, which proves that the ZnO structure was not destroyed in the conjugation reaction. It is known that the conjugation reaction usually takes place between one of the two FA carboxyl groups (γ -carboxyl group at the end of the FA molecule) and a primary amine group from another molecule [34], as shown in scheme 1. This reaction mechanism can be proved by the IR analyses in figure 3. In the ZnO-NH₂ sample, the polymer coating on the ZnO surfaces was confirmed by the IR bands at 1722 and 2876 cm⁻¹, which were from the C=O and C-H groups of the monomers. The two bands at 3400 and 1583 cm⁻¹ [21], corresponding to the N-H stretching vibration and NH₂ bending mode of the free NH₂ groups, respectively, proved that primary amine groups had been grafted onto the ZnO surfaces. After FA conjugation, both the N-H bending mode of the free NH₂ groups in ZnO-NH₂ QDs at 1583 cm⁻¹ and the O-H stretching of COOH in FA at 3142 cm⁻¹ disappear together in the ZnO-FA sample [22]. In the meantime, the characteristic FA band of the ν (N-H) amide II vibration is observed in the ZnO-FA sample at 1605 cm⁻¹, while other characteristic FA peaks are unaltered in the ZnO-FA sample, indicating that the FA structure is not damaged after conjugation.

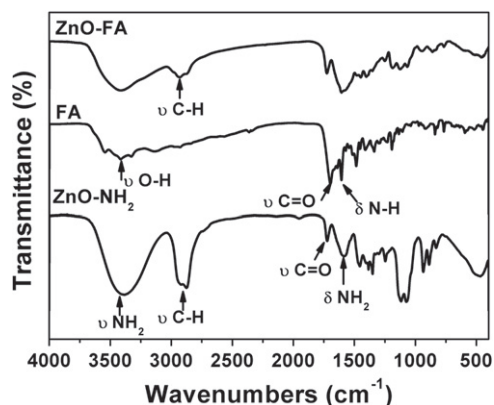


Figure 3. FTIR spectra of ZnO-FA, FA, and ZnO-NH₂ in KBr pellets.

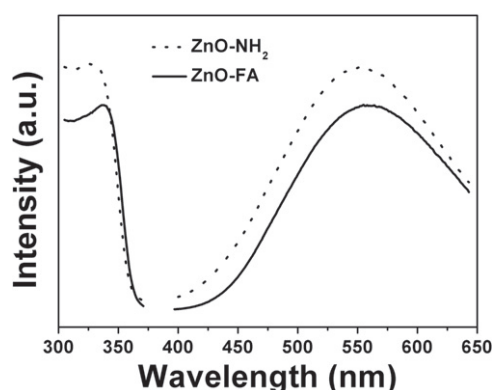


Figure 4. PL excitation and emission spectra of ZnO-NH₂ QDs (dotted lines) and ZnO-FA QDs (solid lines).

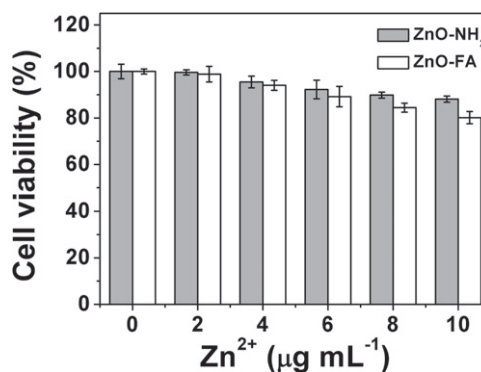


Figure 5. Cell viability resulting from MTT assays measurements on MCF-7 cells incubated with ZnO-NH₂ and ZnO-FA for 24 h, respectively.

The photoluminescent (PL) emission of ZnO-NH₂ QDs is around 554 nm, which is the typical luminescence related with ZnO surface defects (figure 4). The PL emission of ZnO did not change significantly when FA was grafted onto ZnO, because the conjugation reaction was carried out carefully at moderate conditions, and the copolymer shells had protected the ZnO cores tightly. The method of coating polymer is critical in protecting the visible fluorescence of ZnO QDs. For example, Sun *et al* [35] mixed ZnO QDs with α -zirconium phosphate nanoplatelets and poly(methylmethacrylate)

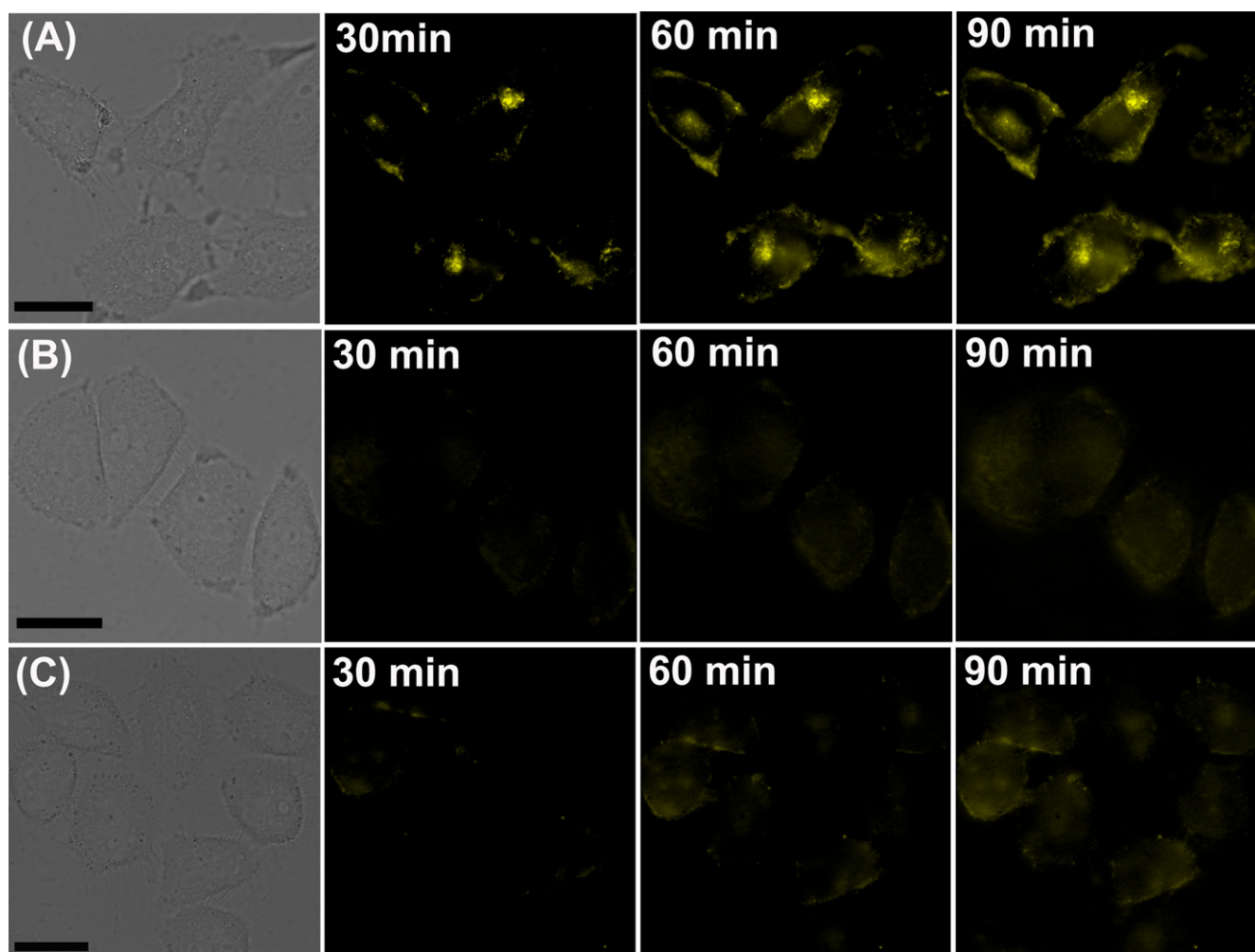


Figure 6. Confocal luminescence images of MCF-7 cells incubated with (A) ZnO-FA, and (B) ZnO-NH₂ at different time intervals, respectively. (C) Confocal luminescence images of 293T cells incubated with ZnO-FA at different time intervals. The left column is under bright field, while the other images were obtained under UV light.

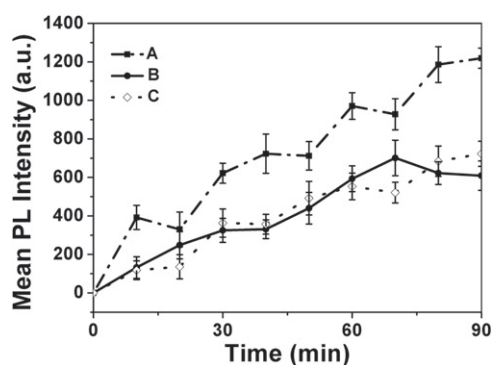


Figure 7. PL intensity evolutions of (A) MCF-7 cells treated with ZnO-FA, (B) MCF-7 cells treated with ZnO-NH₂, and (C) 293T cells treated with ZnO-FA.

(PMMA) in acetone to cast films with both UV emission and visible luminescence, but when the films were dried at 120 °C, the visible luminescence of the ZnO QDs was quenched, because the ZnO surface defects were passivated by the PMMA. If some polymers cannot suppress ZnO QD

aggregation effectively, ZnO visible emission can also be quenched. In our previous research, polyethylene oxide and ZnO nanoparticles were mixed in solvents and evaporated to be composite films. When the ZnO content increased, the nanoparticles aggregated more and more heavily, and the ZnO visible emission intensity decreased gradually [36, 37]. In this work, ZnO QDs were coated tightly by a copolymer shell through the *in situ* polymerization on the ZnO surface. In the well-designed copolymer shell, the inside hydrophobic layer prevented water attack towards the luminescent centers on the ZnO surface, and the outside hydrophilic groups made ZnO QDs dispersed homogeneously in water. Thus the subsequent conjugation with FA did not damage the luminescence of ZnO QDs.

Cytotoxicity is one of the most important assessment criteria for evaluating biomaterials before cell experiments, which is typically measured by the MTT assays. In figure 5, the cell vitality results confirmed that both ZnO-NH₂ and ZnO-FA were almost nontoxic to MCF-7 cells. After incubation with these QDs for 24 h, more than 80% of the MCF-7 cells survived when the corresponding concentration of Zn²⁺

ions was less than $10 \mu\text{g mL}^{-1}$. It is interesting that the cytotoxicity of the ZnO-FA QDs towards MCF-7 cells was higher than ZnO-NH₂ QDs to the same cells. According to our previous research [21], although ZnO QDs are less toxic than many other semiconductor QDs, excess Zn²⁺ ions resulting from ZnO decomposition in cells and the related ROS (reactive oxygen species) showed considerable cytotoxicity in MTT assays. Therefore, the enhanced cytotoxicity of ZnO-FA QDs towards MCF-7 cells can be ascribed to the FA conjugation, which promoted the cellular uptake amount of ZnO-FA QDs and resulted in higher concentrations of Zn²⁺ ions and ROS in cells. In a previous work, Zhao *et al* [16] also demonstrated that FA had a high affinity to FA-receptor (FR) and resulted in the preferential accumulation of the γ -cyclodextrin-folate complex-functionalized CdSe quantum dots in FR-positive tumor cells, inducing the enhancement of the cytotoxicity towards the FR-positive tumor cells.

FA has been widely conjugated with nanoparticles for biological applications, but several issues in this area should be addressed. One is the mostly reported FA-QDs are Cd-related QDs, while the Cd element has been proved toxic to both animals and cells [37, 38]. Another is that many FA-modified nanoparticles are larger than 15 nm, so they cannot be cleared by the kidney. For example, Chan *et al* grafted FA and the anticancer drug camptothecin (CPT) onto the EuGd-MSN surface to give multifunctional mesoporous silica nanoparticles (EuGd-SS-CPT-FA-MSNs) for *in vitro* and *in vivo* dual-mode imaging, theranostics, and targeted tracking. However, the decomposition or excretion of such over 110 nm-sized nanoparticles remained a problem [39]. In contrast, ZnO QDs seem to overcome the above-mentioned drawbacks, because ZnO QDs have lower cytotoxicity and smaller sizes; most importantly, ZnO QDs can be biodegraded and excreted easily by animals. In fact, there are few reports concerning target bio-imaging by FA-modified ZnO QDs so far, because it is really difficult to synthesize such material with strong and stable luminescence. In the present research, we successfully synthesized the stable ZnO-NH₂ QDs as the precursors. Since the ZnO cores were protected by the polymer shells, the FA conjugation did not damage the fluorescence, which arose from the ZnO surface defects. Thus the ZnO-FA QDs could be employed as the specific fluorescent probes for cancer cells.

It is known that the human breast carcinoma cells MCF-7 possess many FA receptors on the membrane, while the human embryonic kidney cells 293T do not. So we compared the cellular uptaking processes of ZnO-FA QDs, employing the FR-positive breast cancer cells MCF-7 and the FR-negative embryonic kidney cells 293T at different time intervals. Under a CLSM, all imaging profiles in figure 6 exhibit gradually increased fluorescent intensities, indicating that the QDs uptaken by cells are inevitable. But the profile composed of ZnO-FA QDs and MCF-7 cells (figure 6(a)) exhibits the strongest fluorescence throughout the procedure, which suggests that the interactions of FA groups on ZnO QDs and FA receptors on MCF-7 cell membranes significantly facilitate the endocytosis of ZnO-FA into the cells. The profile composed of ZnO-NH₂ QDs and MCF-7 cells (figure 6(b)) and

the profile composed of ZnO-FA QDs and 293T cells (figure 6(c)) show much weaker fluorescence, which proves that specific recognition takes place only when both FA and FA receptor coexist in the cell culture environment. To observe such recognition more clearly, the fluorescent intensity variations of different profiles are compared in figure 7. The PL intensity of the MCF-7 cells treated with ZnO-FA is higher than the MCF-7 cells treated with ZnO-NH₂ and the 293T cells treated with ZnO-FA throughout the procedure, in accordance with figure 6. Therefore, the ZnO-FA QDs can be utilized as targeted fluorescent probes for the diagnosis of FR-positive cancer cells *in vitro*.

4. Conclusion

Among the numerous reports concerning luminescent QDs and cell imaging experiments, our present research has made progress in two aspects. One is successfully grafting FA onto ZnO QD surfaces to obtain aqueous stable colloids with strong fluorescence. The other is employing such ZnO-FA QDs as fluorescent probes to recognize cancer cells with overexpressed FA receptors so as to differentiate cancer cells from the normal ones. Such progress is ascribed to the critically controlled synthetic conditions and the well-designed structure of the core-shell QDs. In future work, ZnO-FA QDs will be developed as novel nanocarriers that deliver anticancer drugs in solid tumors for killing cancer cells specifically.

Acknowledgments

This work was supported by the National Basic Research Program of China (2013CB934101), the National Natural Science Foundation of China (21271045), and NCET-11-0115.

References

- [1] Umar A, Dunn B K and Greenwald P 2012 Future directions in cancer prevention *Nat. Rev. Cancer* **12** 835–48
- [2] Thompson I M, Cabang A B and Wargovich M J 2014 Future directions in the prevention of prostate cancer *Nat. Rev. Clin. Oncol.* **11** 49–60
- [3] Dreves J *et al* 2005 Soluble markers for the assessment of biological activity with PTK787/ZK 222584 (PTK/ZK), a vascular endothelial growth factor receptor (VEGFR) tyrosine kinase inhibitor in patients with advanced colorectal cancer from two phase I trials *Ann. Oncol.* **16** 558–65
- [4] Shimizu K *et al* 2004 Suppression of VEGFR-3 signaling inhibits lymph node metastasis in gastric cancer *Cancer. Sci.* **95** 328–33
- [5] Paez J G *et al* 2004 EGFR mutations in lung cancer: correlation with clinical response to gefitinib therapy *Science* **304** 1497–500
- [6] Valtola R, Salven P, Heikkilä P, Taipale J, Joensuu H, Rehn M, Pihlajaniemi T, Weich H, DeWaal R and Alitalo K 1999 VEGFR-3 and its ligand VEGF-C are associated with angiogenesis in breast cancer *Am. J. Pathol.* **154** 1381–90

- [7] Peng X H, Cao Z H, Xia J T, Carlson G W, Lewis M M, Wood W C and Yang L 2005 Real-time detection of gene expression in cancer cells using molecular beacon imaging: new strategies for cancer research *Cancer. Res.* **65** 1909–17
- [8] Gilles C, Polette M, Piette J, Munaut C, Thompson E W, Birembaut P and Foidart J M 1996 High level of MT-MMP expression is associated with invasiveness of cervical cancer cells *Int. J. Cancer.* **65** 209–13
- [9] van Dam G M et al 2011 Intraoperative tumor-specific fluorescence imaging in ovarian cancer by folate receptor- α targeting: first in-human results *Nat. Med.* **17** 1315–9
- [10] Weitman S D, Lark R H, Coney L R, Fort D W, Frasca V, Zurawski V R and Kamem B A 1992 Distribution of the folate receptor GP38 in normal and malignant-cell lines and tissues *Cancer. Res.* **52** 3396–401
- [11] Sun L N, Wei Z W, Chen H G, Liu J T, Guo J J, Cao M, Wen T Q and Shi L Y 2014 Folic acid-functionalized up-conversion nanoparticles: toxicity studies *in vivo* and *in vitro* and targeted imaging applications *Nanoscale* **6** 8878–83
- [12] Zheng M B, Gong P, Zheng C F, Zhao P F, Luo Z Y, Ma Y F and Cai L T 2015 Lipid-polymer nanoparticles for folate-receptor targeting delivery of doxorubicin *J. Nanosci. Nanotechnol.* **15** 4792–8
- [13] Qi L S, Guo Y Y, Luan J J, Zhang D R, Zhao Z X and Luan Y X 2014 Folate-modified beaxarotene-loaded bovine serum albumin nanoparticles as a promising tumor-targeting delivery system *J. Mater. Chem. B* **2** 8361–71
- [14] Zhang Z Y, Zhang P, Guo K, Liang G H, Chen H, Liu B H and Kong J L 2011 Facile synthesis of fluorescent Au@SiO₂ nanocomposites for application in cellular imaging *Talanta* **85** 2695–9
- [15] Patra C R, Bhattacharya R and Mukherjee P 2010 Fabrication and functional characterization of goldnanoparticles for potential application in ovarian cancer *J. Mater. Chem.* **20** 547–54
- [16] Zhao M, Huang H, Xia Q, Ji L and Mao Z 2011 γ -Cyclodextrin–folate complex-functionalized quantum dots for tumor-targeting and site-specific labeling *J. Mater. Chem.* **21** 10290–7
- [17] Manzoor K, Johnny S, Thomas D, Setua S, Menon D and Nair S 2009 Bio-conjugated luminescent quantum dots of doped ZnS: a cyto-friendly system for targeted cancer imaging *Nanotechnology* **20** 065102
- [18] Setua S, Menon D, Asok A, Nair S and Koyakutty M 2010 Folate receptor targeted, rare-earth oxide nanocrystals for bi-modal fluorescence and magnetic imaging of cancer cells *Biomaterials* **31** 714–29
- [19] Cao T Y, Yang Y, Gao Y A, Zhou J, Li Z Q and Li F Y 2011 High-quality water-soluble and surface-functionalized upconversion nanocrystals as luminescent probes for bioimaging *Biomaterials* **32** 2959–68
- [20] Xiong H M, Xu Y, Ren Q G and Xia Y Y 2008 Stable aqueous ZnO@polymer core–shell nanoparticles with tunable photoluminescence and their application in cell imaging *J. Am. Chem. Soc.* **130** 7522–3
- [21] Zhang H J, Xiong H M, Ren Q G, Xia Y Y and Kong J L 2012 ZnO@silica core–shell nanoparticles with remarkable luminescence and stability in cell imaging *J. Mater. Chem.* **22** 13159–65
- [22] Muhammad F, Guo M Y, Guo Y J, Qi W X, Qu F Y, Sun F X, Zhao H J and Zhu G S 2011 Acid degradable ZnO quantum dots as a platform for targeted delivery of an anticancer drug *J. Mater. Chem.* **21** 13406–12
- [23] Zhang Z Z, Xu Y D, Ma Y Y, Qiu L L, Wang Y, Kong J L and Xiong H M 2013 Biodegradable ZnO@polymer core–shell nanocarriers: pH-triggered release of doxorubicin *in vitro* *Angew. Chem. Int. Ed.* **52** 4127–31
- [24] Bai X Y, Li L L, Liu H Y, Tan L F, Liu T L and Meng X W 2015 Solvothermal synthesis of ZnO nanoparticles and anti-infection application *in vivo* *ACS Appl. Mater. Interfaces* **7** 1308–17
- [25] Roy R, Kumar D, Sharma A, Gupta P, Chaudhari S P, Tripathi A, Das M and Dwivedi P D 2014 ZnO nanoparticles induced adjuvant effect via toll-like receptors and Src signaling in Balb/c mice *Toxicol. Lett.* **230** 421–33
- [26] Aal N A, Al-Hazmi F, Al-Ghamdi A A, Al-Ghamdi A A, El-Tantawy F and Yakuphanoglu F 2015 Novel rapid synthesis of zinc oxide nanotubes via hydrothermal technique and antibacterial properties *Spectrochim Acta A* **135** 871–7
- [27] Ozkan E, Ozkan F T, Allan E and Parkin I P 2015 The use of zinc oxide nanoparticles to enhance the antibacterial properties of light-activated polydimethylsiloxane containing crystal violet *RSC Adv.* **5** 8806–13
- [28] Hsu S H, Lin Y Y, Huang S, Lem K W, Nguyen D H and Lee D S 2013 Synthesis of water-dispersible zinc oxide quantum dots with antibacterial activity and low cytotoxicity for cell labeling *Nanotechnology* **24** 475102
- [29] Xiong H M 2010 Photoluminescent ZnO nanoparticles modified by polymers *J. Mater. Chem.* **20** 4251–62
- [30] Fu Y S, Du X W, Kulinich S A, Qiu J S, Qin W J, Li R, Sun J and Liu J 2007 Stable aqueous dispersion of ZnO quantum dots with strong blue emission via simple solution route *J. Am. Chem. Soc.* **129** 16029–33
- [31] Wu Y L, Lim C S, Fu S, Tok A, Lau H M, Boey F and Zeng X T 2007 Surface modifications of ZnO quantum dots for bio-imaging *Nanotechnology* **18** 215604
- [32] Song E Q, Zhang Z L, Luo Q Y, Lu W, Shi Y B and Pang D W 2009 Tumor cell targeting using folate-conjugated fluorescent quantum dots and receptor-mediated endocytosis *Clin. Chem.* **55** 955–63
- [33] Zhao Y L, Liu S, Li Y P, Jiang W, Chang Y L, Pan S, Fang X X, Wang Y A and Wang J Y 2010 Synthesis and grafting of folate-PEG-PAMAM conjugates onto quantum dots for selective targeting of folate-receptor-positive tumor cells *J. Colloid. Interf. Sci.* **350** 44–50
- [34] Zhao Y L, Liu S, Li Y P, Jiang W, Chang Y L, Pan S, Fang X X, Wang Y A and Wang J Y 2010 Synthesis and grafting of folate-PEG-PAMAM conjugates onto quantum dots for selective targeting of folate-receptor-positive tumor cells *J. Colloid. Interf. Sci.* **350** 44–50
- [35] Sun D Z and Sue H J 2009 Tunable ultraviolet emission of ZnO quantum dots in transparent poly(methyl methacrylate) *Appl. Phys. Lett.* **94** 253106
- [36] Xiong H M, Zhao X and Chen J S 2001 New polymer-inorganic nanocomposites: PEO-ZnO and PEO-ZnO-LiClO₄ films *J. Phys. Chem. B* **105** 10169–74
- [37] Cho S J, Maysinger D, Jain M, Roder B, Hackbarth S and Winnik F M 2007 Long-term exposure to CdTe quantum dots causes functional impairments in live cells *Langmuir* **23** 1974–80
- [38] Resch-Genger U, Grabolle M, Cavaliere-Jaricot S, Nitschke R and Nann T 2008 Quantum dots versus organic dyes as fluorescent labels *Nat. Methods* **5** 763–75
- [39] Zhang L E, Zeng L Y, Pan Y W, Luo S, Ren W Z, Gong A, Ma X H, Liang H Z, Lu G M and Wu A G 2015 Inorganic photosensitizer coupled Gd-based upconversion luminescent nanocomposites for *in vivo* magnetic resonance imaging and near-infrared-responsive photodynamic therapy in cancers *Biomaterials* **44** 82–90